



## Full Length Article

# Multi-functional plasmonic fabrics: A flexible SERS substrate and anti-counterfeiting security labels with tunable encoding information

Sijia Liu<sup>a</sup>, Xiaoran Tian<sup>a</sup>, Jiaqi Guo<sup>b</sup>, Xianming Kong<sup>a,\*</sup>, Lingzi Xu<sup>a</sup>, Qian Yu<sup>a,\*</sup>, Alan X. Wang<sup>c</sup>

<sup>a</sup> School of Petrochemical Engineering, Liaoning Petrochemical University, Fushun, Liaoning 113001, PR China

<sup>b</sup> Jiangsu Co-Innovation Center for Efficient Processing and Utilization of Forest Resources and Joint International Research Lab of Lignocellulosic Functional Materials, Nanjing Forestry University, Nanjing 210037, PR China

<sup>c</sup> School of Electrical Engineering and Computer Science, Oregon State University, Corvallis, OR 97331, USA

## ARTICLE INFO

## Keywords:

SERS  
Plasmonic cotton gauze  
In-situ growth  
Anti-counterfeiting  
Tunable encoding information

## ABSTRACT

Multi-functional plasmonic fabric comprised of silver nanoparticles (Ag NPs) and cotton gauze was fabricated through an in-situ growth method. Ag NPs with high density were immobilized on the surface of cotton fibers. The plasmonic cotton gauze exhibits excellent flexible features, temporal stability and SERS enhancement factors close to  $10^5 \times$ . The plasmonic cotton gauze was labelled with multiplexed Raman probes and used for anti-counterfeiting applications. The encoding information could be readily changed by adjusting the ratio between components in the mixture of Raman probe molecules. This novel strategy could create rich Raman information based on the combination of a few Raman probes, which significantly increases the security levels in anti-counterfeiting. The plasmonic cotton gauze was also employed as a flexible SERS substrate for sensing pesticide from irregular surfaces of orange by a simple swiping process.

## 1. Introduction

Surface-enhanced Raman scattering (SERS) is a spectroscopic technique that provides molecular structural information in an instant, sensitive and accurate way. Furthermore, the measurement process is non-destructive and anti-interference with water, which enables wide applications in surface science, biochemistry, forensics, food safety, medical diagnosis, and catalysis science [1-7]. The SERS substrate plays a pivotal role in many practical applications [8,9]. However, most existing SERS substrates are rigid plates such as glass or quartz, which limit their applications for sensing analytes from uneven or rugged surfaces. Thus, the development of soft SERS substrates could expand the potential of SERS sensing into new regimes.

Recently, different soft materials including polymers[10], papers [11], cotton swabs[12] and cellulose fibers[13], have been used as flexible SERS substrates. Cotton is the most abundant natural fiber as a raw material for producing clothes and textiles. Cotton based SERS substrates have attracted considerable interests due to the high mechanical flexibility, good permeability, eco-friendly and cost-effective properties [14]. Ge and co-workers decorated the surface of natural woven cotton fabrics with Ag NPs through electrostatic self-assembly, in which the limit of detection of PATP by the soft SERS substrate achieved

$10^{-7}$  M [15]. Fan's group developed a SERS Q-tip platform by depositing Ag NPs onto the surface of cotton swabs, which showed great performance in detecting explosives at trace level ( $1.2 \text{ ng/cm}^2$ ) [2]. Our group has fabricated flexible plasmonic fibers by assembling Ag NPs on the surface of regenerated cellulose fibers and the composite was successfully used for adsorbing and sensing bisphenol A from fruit juice [16]. The ionic liquid is needed in the fabrication process of regenerated cellulose fibers, which limited the batch preparation of fiber. The plasmonic cotton fabrics can be pasted or sewn onto the surface of packages, which brings opportunity for anti-counterfeiting.

For centuries, counterfeited and pirated goods have caused enormous economic losses and great threats to consumers, organizations and the society [17]. Security label is a direct, cost-effective, easy to use technology in anti-counterfeiting. Many security labels have been widely adopted in checks, credit cards, cash bills, and packages of goods. The power or thermal dependent multicolor upconversion nanoparticles were proposed and printed on the package, which are advanced anti-counterfeiting materials[18-21]. The thermal upconversion nanoparticle is difficult used in plastic packages as the high working temperature, and the preparation of lanthanide-doped energy cascade nanoparticles is complicated. Plasmonic materials show great potentials as a new generation of security labels [22-25]. The small dimensions and

\* Corresponding authors.

E-mail addresses: [xmkong@lnpu.edu.cn](mailto:xmkong@lnpu.edu.cn) (X. Kong), [qyu@lnpu.edu.cn](mailto:qyu@lnpu.edu.cn) (Q. Yu).

<https://doi.org/10.1016/j.apsusc.2021.150861>

Received 11 March 2021; Received in revised form 1 August 2021; Accepted 4 August 2021

Available online 8 August 2021

0169-4332/© 2021 Elsevier B.V. All rights reserved.

tunable optical properties of plasmonic materials could encode high density optoelectronic information that can be read out by various optical instruments. The combination of plasmonic materials with SERS exhibit an effective way to construct security labels as SERS spectra present unique vibrational fingerprints of molecules with narrow peaks enhanced by plasmonic nanostructures. The cotton fabrics is an ideal SERS security label for anti-counterfeiting. First, the encoding security information is sufficiently unique as it comes from the label molecules [26,27]. Second, cotton is abundant from nature and is eco-friendly and cost-effective [28]. Last but not the least, the soft cotton fabrics can be cut into any shape while keeping their mechanical flexibility, which is suitable for irregular surfaces. The SERS information produced by the security label depends on the Raman probes labelled on the surface of the plasmonic substrate. Generally, a single Raman probe is used to generate the anti-counterfeiting SERS spectra, which restricts the diversity of spectral information and is not sufficient to prevent them from being duplicated. The multiple labeled molecules can be deposited by different layers or arrays to enhance the security level. However, the fabrication process of multi-layer materials is complicated, time consuming and the special facilities are necessary.

Herein, we propose a novel strategy to fabricate effective security labels with good flexibility and tunable encoding information. The Raman probe molecules with thiol group could bond to the surface of Ag NPs through chemical reaction. More importantly, the encoding information of the anti-counterfeiting security labels can be easily tuned by changing the ratio between two Raman probe molecules modified on the Ag NPs, in which the abundant SERS information was obtained only from two kinds of Raman probe molecules. The authors demonstrate the method for fabricating flexible SERS security labels by decorating Ag NPs on cotton gauze by in-situ growth process. Then the two kinds of Raman probe molecules were labeled on the plasmonic cotton gauze, which is denoted as anti-counterfeiting SERS security labels. The construction procedure is shown in Scheme 1. Additionally, the plasmonic cotton gauze is an effective SERS substrate, which is utilized for detecting pesticide residues from the surface of orange by simple swabbing.

## 2. Experimental

### 2.1. Materials and chemicals

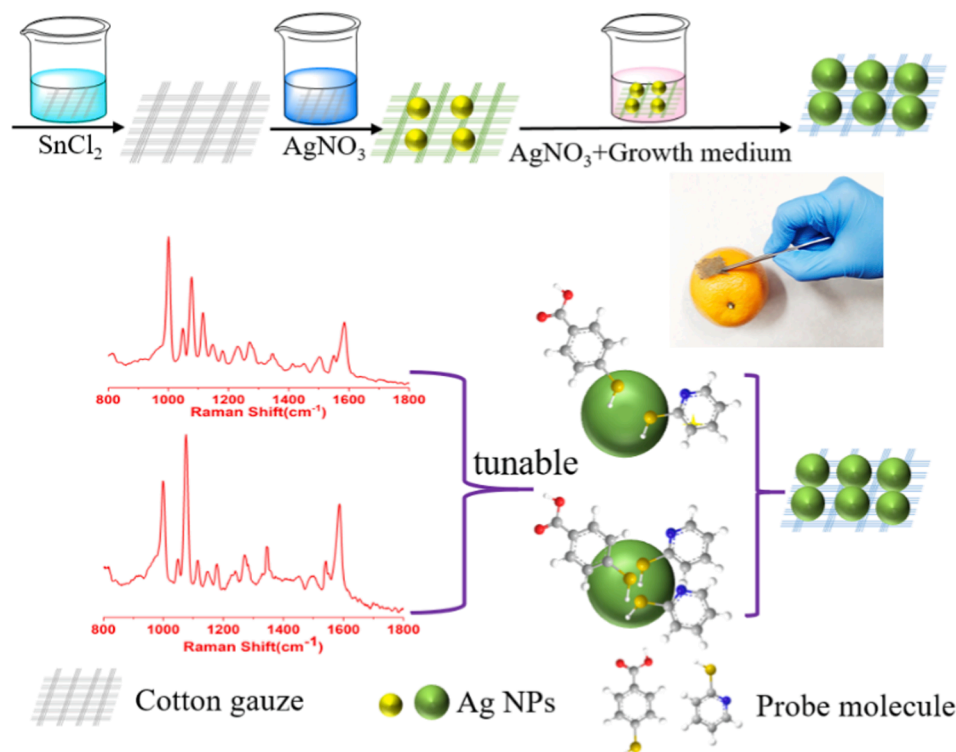
L-Ascorbic acid (AA) and Tin (II) chloride dihydrate ( $\text{SnCl}_2$ ) were purchased from Sinopharm Chemical Reagent Co., Ltd (China). Silver nitrate ( $\text{AgNO}_3$ ), 2-Mercaptopyridine(2-MPY) and 4-Mercaptobenzoic acid (4-MBA) was obtained from Aladdin (Shanghai, China). Pyrimethanil and p-Aminothiopheno (PATP) was obtained from Innochem (Beijing, China). Cotton gauze was supplied by Hualu textile Co., Ltd (Shandong, China). All reagents used in the experiment were analytical grade and without further purification.

### 2.2. Fabrication of plasmonic cotton gauze

The plasmonic cotton gauze was fabricated through in-situ growth Ag NPs on the surface of cotton gauze. The cotton gauze was firstly immersed in an aqueous solution of stannous chloride (20 mM) and HCl (20 mM) for 10 min to deposit  $\text{Sn}^{2+}$  on the surface of cotton. The pre-treated cotton gauze was washed sequentially with Milli-Q water and acetone, and then dried by nitrogen flow. Then it was soaked in 20 mM silver nitrates for 10 min to deposit Ag seeds onto the surface of the cotton gauze. After repeating the process three times, the cotton gauze with Ag seeds was dipped in 1.5 mL growth media ( $\text{AgNO}_3$  with concentrations at 5 mM, 10 mM, 15 mM and 20 mM, with 20 mM ascorbic acid) for 10 min, which enables in-situ growth of Ag NPs into bigger size. Then the cotton gauze was removed from the solution and washed with Milli-Q water after 1 min.

### 2.3. Construction of anti-counterfeiting SERS security labels

The standard solution (10 mM) of MBA, 2-MPY, PATP and 2-MPY was prepared respectively. The mixture 1(MBA /2-MPY, 1/1) and mixture 2(PATP/2-MPY, 1/1) were used as beacon molecules decorating the plasmonic cotton gauze. The cotton gauze-Ag NPs were immersed into the solution of beacon molecules at 0.1 mM concentration for 20



**Scheme 1.** Illustration of fabrication of plasmonic cotton gauze used for SERS sensing and anti-counterfeiting.

min. The encoding information of the anti-counterfeiting SERS security labels (plasmonic cotton gauze) were adjusted by change the ratio between the two Raman probe molecules in mixture.

#### 2.4. Characterization

Scanning electron microscope (SEM) images were acquired by a SU8010 field-emission scanning electron microscope (Hitachi, Japan). Transmission electron microscopy (TEM) images and electron diffraction (SAED) patterns were collected by a JEM-2100FS electron microscope (JEOL, Japan). The X-ray diffraction (XRD) patterns of cotton gauze before and after Ag deposition were collected by a SmartLab x-ray diffractometer (Rigaku Japan). The cotton gauze samples were first pressed to pellets (1 cm in diameter) for X-Ray spectra measurements.

#### 2.5. SERS measurement

The SERS enhancement effect of the plasmonic cotton gauze was evaluated by using MBA as the Raman probe molecule. The cotton gauze-Ag substrate was dipped into aqueous solution of MBA with different concentrations for 3 min, and then dried in air. The Raman measurement was conducted using a portable Raman spectrometer (BWS465 iRaman from B&W Tek, USA) with a 785 nm wavelength excitation laser. The diameter of the beam spot was 105  $\mu\text{m}$ . A 1.5 m bifurcated fiber probe was used to illuminate the sample and collected Raman signals with 40% power and 1 sec acquisition time. All Raman spectra were collected in the range from 300 to 3000  $\text{cm}^{-1}$ . The data were processed with BWSPEC software. For SERS sensing of pesticides

from oranges, the pyrimethanil solution at different concentrations were sprayed onto the surface of oranges. The cotton gauze (10 mg) simply swabbed the surface of the orange (2 cm  $\times$  2 cm), followed by Raman measurement.

### 3. Results and discussion

#### 3.1. Characterization of the plasmonic cotton gauze

The Ag NPs on cotton using a seed-mediated electroless deposition process. Ag seeds were deposited on the surface of cotton gauze by an electroless reduction of  $\text{Ag}^+$  by  $\text{Sn}^{2+}$ . A secondary growth step was carefully controlled by using a gentle reducing agent,  $\text{SnCl}_2$ , which also provided adhesion to anchor the Ag NPs to the surface of cotton gauze. The surface morphology of the cotton gauze before and after Ag deposition via SEM and TEM. As shown in Fig. 1a, the raw cotton fiber presents a clean surface and with diameters near 20  $\mu\text{m}$ . After the cotton gauze was soaked in the solution of  $\text{SnCl}_2$  and  $\text{AgNO}_3$ , the Ag seeds with small size were immobilized on the surface of the cotton fibers (Figure S1). The appearance of the cotton fiber exhibits slight roughness as shown in Fig. 1b, which indicates that the Ag NPs were successfully prepared by the reduction of  $\text{Sn}^{2+}$ . Four different concentrations of  $\text{AgNO}_3$  (5 mM, 10 mM, 15 mM and 20 mM) were adjusted in the growth media for in-situ growth of Ag NPs on the cotton fiber. The SEM images of Ag NPs deposited at different conditions were presented in Figure S2. As shown in Figure S2a, the diameter of Ag NPs is between 30 and 40 nm corresponding to 5 mM of  $\text{AgNO}_3$  solution used in the growth media. The SEM image in Fig. 1c shows that the Ag NPs

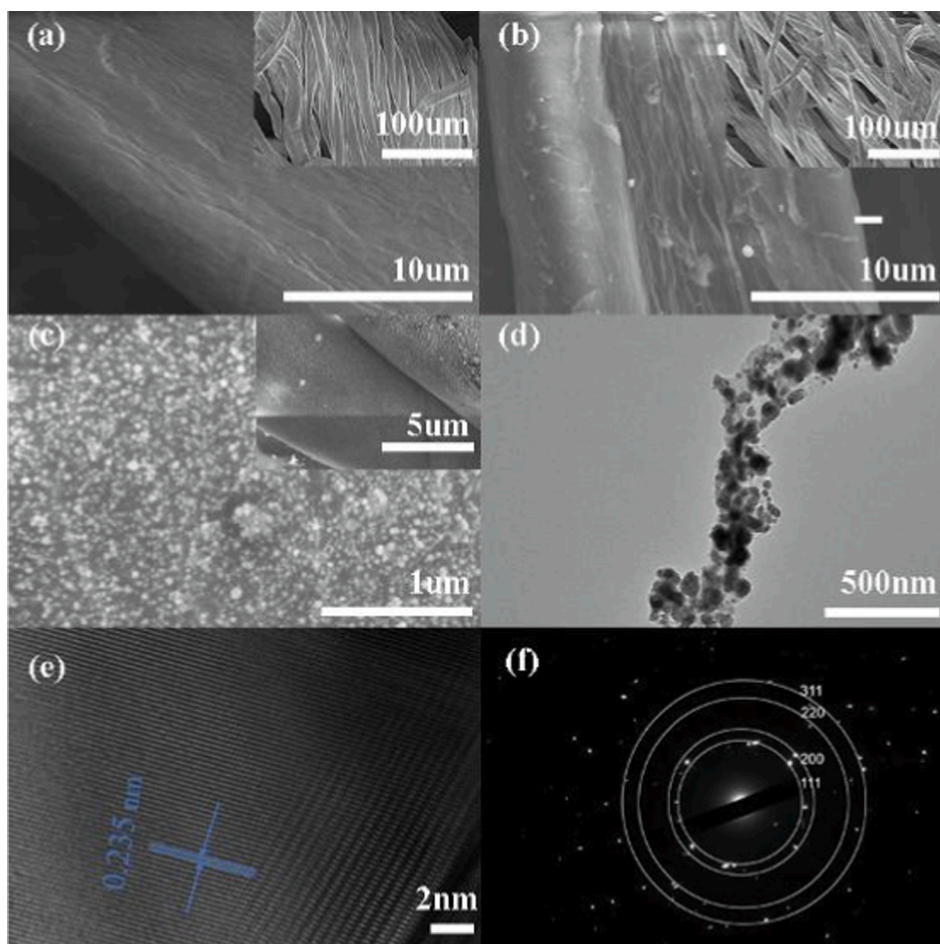


**Fig. 1.** SEM images of cotton gauze before (a) and after (b, c) Ag NPs deposition, TEM images of Ag NPs on the cotton gauze (d, e) and SAED patterns of Ag NP on cotton gauze(f).

grew to bigger diameters from seeds on cotton fibers by dipping them into the growth media with 10 mM  $\text{AgNO}_3$  solution. The Ag NPs were densely and uniformly distributed on the surface of cotton fibers. The TEM image was employed to determine the size distribution of Ag NPs on the cotton gauze as shown in Fig. 1d. It is clearly seen that the size of Ag NPs ranges from 50 to 70 nm, and the Ag NPs were immobilized on the surface of the cotton fibers. In order to investigate the microstructure of Ag NPs in more details, the high-resolution transmission electron microscopy (HRTEM) was used. The HRTEM image of randomly selected Ag NPs was shown in Fig. 1e. The examined Ag NPs exhibit face-centered cubic (FCC) lattice with pure Ag (111) interlayer spacing at 0.225 nm [29]. Fig. 1f is the SAED pattern measured from a single Ag NP, in which a series of diffraction rings were observed, indicating that the Ag NP crystal is polycrystalline. As the concentration of  $\text{AgNO}_3$  solution increased to 15 mM, the diameter of Ag NPs increased to nearly 100 nm and bigger clusters of Ag NPs were formed as shown in Figure S2b. Also an Ag shell was formed on the surface of fiber as the concentration of  $\text{AgNO}_3$  increased to 15 mM.

The SERS enhancement effect of the cotton gauze-Ag was evaluated using 4-MBA as the Raman probe molecule. The SERS spectra of MBA on the cotton gauze-Ag fabricated through different conditions was shown in Figure S3, in which the substrate in-situ growth with 10 mM  $\text{AgNO}_3$  shows the highest SERS enhancement. Fig. 2 shows the SERS spectra of 4-MBA ( $10^{-4}$  M) from the flexible cotton gauze-Ag and rigid glass-Ag. The prominent Raman peaks of MBA on the plasmonic cotton gauze were observed at 1072 and 1586  $\text{cm}^{-1}$ , which are attributed to the in-plane ring breathing vibration of aromatic ring and totally symmetric vibration of C-C bond [30], respectively. The intensity of Raman signals from the cotton gauze is higher than that from glass. The reason is that flexible cotton could adsorb more analytes on the surface. Based on the intensity of the Raman peak at 1072  $\text{cm}^{-1}$ , the SERS enhancement factor of the cotton gauze-Ag NPs was near  $1.15 \times 10^5$ , indicating excellent SERS activities.

The uniformity of Raman signals from the cotton gauze substrate also plays an important role in practical applications. In order to evaluate the uniformity of SERS spectra from the cotton gauze, the Raman spectra of 4-MBA molecules ( $10^{-5}$  M) were collected from five randomly selected positions on the cotton gauze-Ag as presented in Fig. 3(a). The distribution of the intensity of Raman spectra at 1072  $\text{cm}^{-1}$  was presented in Fig. 3(b). The peak intensity at 1072  $\text{cm}^{-1}$  from five spectra calculated a relative standard deviation (RSD) of 4.4%, indicating a good uniformity of the plasmonic cotton gauze [31]. The excellent uniformity proved that the cotton gauze-Ag NPs substrate is a reliable platform for practical

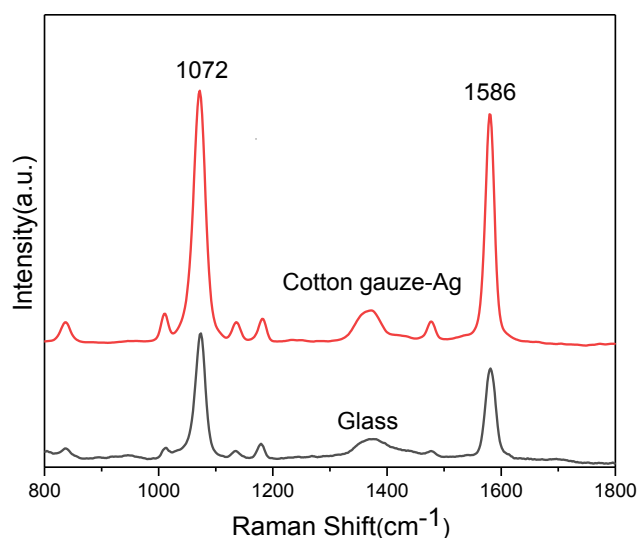


Fig. 2. SERS spectra of 4-MBA ( $10^{-4}$  M) on the cotton gauze and glass substrate.

SERS measurement.

A key feature of the cotton gauze-Ag used as a SERS substrate or anti-counterfeiting security label is the stability. The stability of SERS cotton gauze-Ag was investigated in a period of 50 days at air condition. The SERS spectra of 4-MBA at  $10^{-5}$  M were collected every 10 days as shown in Fig. 3(c). There is only a small degradation over the duration of 50 days as shown in Fig. 3(d). The SERS performance of the cotton gauze-Ag also investigated after washing and friction, in which the friction experiment was simulated by using blank cotton gauze. The SERS spectra of MBA on cotton gauze-Ag after washing and friction were presented in figure S4, which indicated the friction nearly hasn't effect on the signal strength of SERS spectra. These results demonstrate that the cotton gauze-Ag NPs has excellent SERS stability, which enables long-term stability as SERS substrates and anti-counterfeiting SERS security labels.

The phase composition of cotton gauze and cotton gauze-Ag were characterized by XRD spectra as presented in Fig. 4. The XRD spectra of the raw cotton gauze show four intense diffraction peaks at  $2\theta$  of 15.2°, 16.9°, 23.1° and 34.4°, which are assigned to the (1-10), (110), (200) and (004) planes of Cellulose I [32]. After the decoration of Ag NPs on the surface of cotton gauze, four new sharp diffraction peaks were observed at  $2\theta$  values of 38.1°, 44.3°, 64.5°, 77.3° and 81.4°, which are assigned to the (111), (200), (220), and (311) crystal planes of Ag NPs on the cotton gauze according to JCPDS card (No. 04-0783) [33,34]. The XRD results further proved the successful immobilization of Ag NPs on the surface of the cotton gauze. The decrease of the peak intensity of cellulose was due to the coverage of Ag NPs. The Ag NPs on the surface of cotton fiber have not changed the crystal structure of the cotton fiber.

### 3.2. On-site swabbing sensing of pyrimethanil from oranges

Pyrimethanil (PMT) is a kind of anilinopyrimidine pesticides that is usually used for protecting fruits from gray mold. The residue or accumulation of PMT is harmful to the cardiac development [25,35]. SERS has been employed as an efficient method to detect PMT from fruit [36]. In practical SERS applications, the simplest and most convenient way is wiping samples by a SERS substrate directly. The flexible cotton gauze-Ag SERS substrate is suitable for wiping from irregular surfaces. The detailed process of swab detection was demonstrated as follows: 0.2 mL of PMT at different concentrations were sprayed onto the surface of oranges and then swabbed by the cotton gauze-Ag. The Raman spectra measured from the cotton gauze-Ag were shown in Fig. 5. No Raman bands of PMT were observed from the surface of orange without pesticide spraying. Raman peaks were observed after the PMT sprayed onto the surface of oranges. Typical characteristic Raman peaks of PMT were observed at 556  $\text{cm}^{-1}$ , 610  $\text{cm}^{-1}$ , 997  $\text{cm}^{-1}$  and 1232  $\text{cm}^{-1}$ . The intense Raman peak at 997  $\text{cm}^{-1}$  is assigned to the breathing mode of the aromatic ring, the peaks presented at 556  $\text{cm}^{-1}$  and 610  $\text{cm}^{-1}$  were due to the antisymmetric stretching of the NH group, and the peak at 1232  $\text{cm}^{-1}$  is attributed to in-plane deformation vibration of pyrimidine [36]. It was found that there was a smooth polynomial relationship between Raman intensity and the concentration of pyrimethanil on orange (Fig. 5b). The concentration of PMT could be defined through the equation. The recovery test was carried out by the standard addition method as well as the swiping method proposed at here, the results are shown in Table S1. The recovery values of pyrimethanil at different concentration on orange were from 92.8% to 101%. The results indicated that the flexible cotton gauze-Ag possess high SERS sensitivity by direct swabbing detection without additional sample pretreating process.

### 3.3. Anti-counterfeiting SERS security labels with tunable encoding information

4-MBA and 2-MPY are selected as probe molecules anchoring on the surface of the plasmonic cotton gauze. The thiol groups of them could

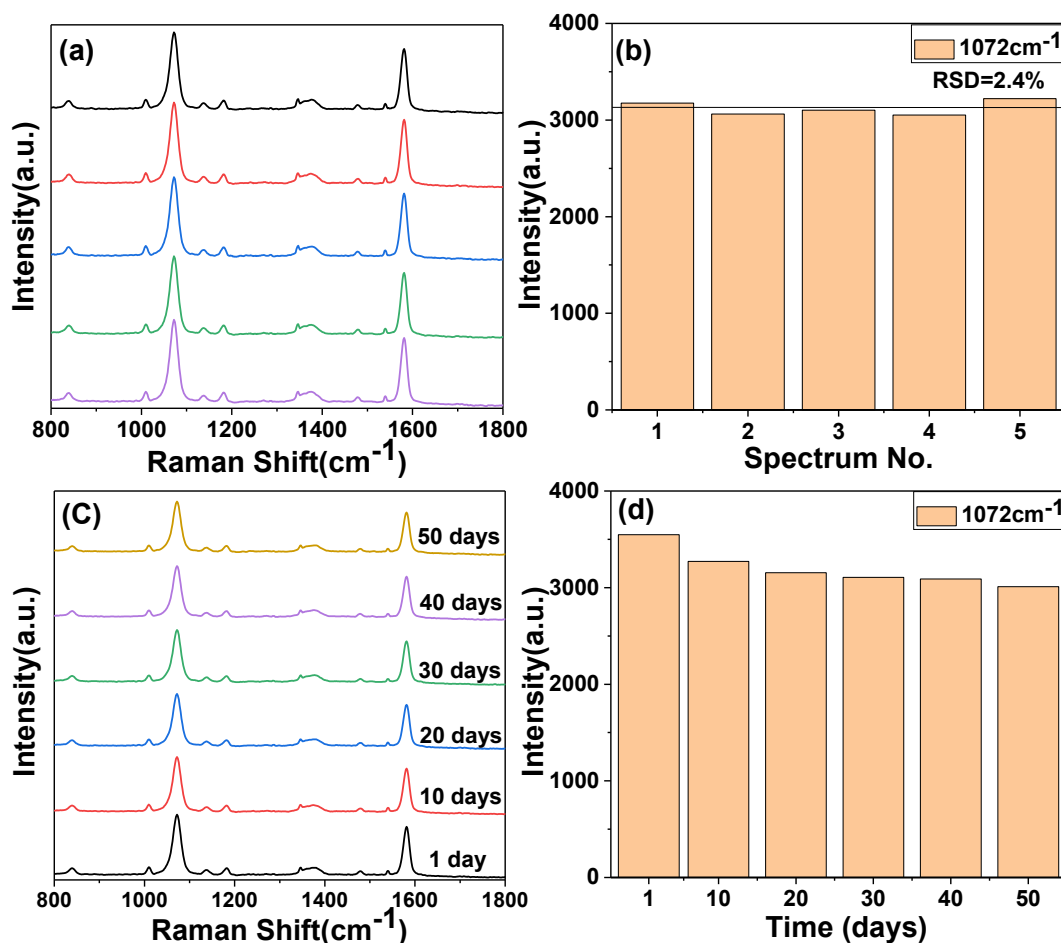


Fig. 3. Raman spectra of MBA ( $1^{-5}$  M) measured from five random spots(a) and different times (b) of the cotton gauze-Ag, and the histogram results of the intensities of peak at the  $1072\text{ cm}^{-1}$  (b) and (d).

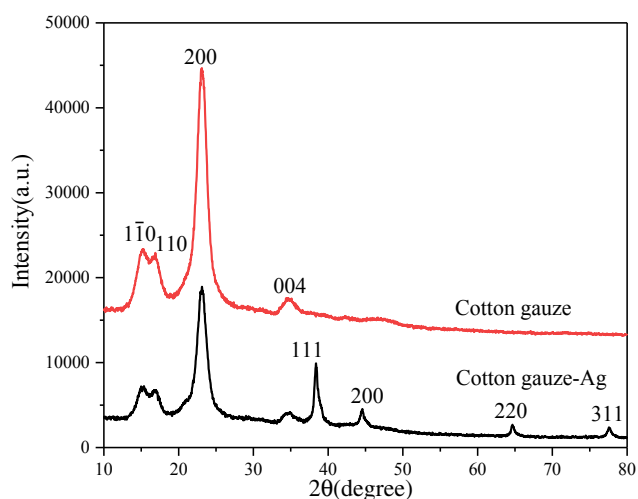


Fig. 4. XRD spectra of cotton gauze and after Ag NPs deposition.

form a self-assembled monolayer on the Ag surface via a metal-thiol chemical bond. The mixture of Raman probe molecules could encrypt the abundant spectra information on the anti-counterfeiting SERS security labels as shown in Fig. 6 (a). The spectra information cannot be directly read out on the physical characteristics of the cotton gauze-Ag, which could be utilized as advanced authentication of the SERS anti-counterfeiting security label. Raman signal of pure 4-MBA and 2-MPY

were collected and presented in Fig. 6(a). For 2-MPY, the most prominent peak at  $999\text{ cm}^{-1}$  is assigned to the vibration of the ring breathing, the peak at  $1080\text{ cm}^{-1}$  is due to the C-H deforming vibration, and the peak at  $1133\text{ cm}^{-1}$  belongs to the C-S stretching vibration. The Raman intensity ratio of the peaks at  $999\text{ cm}^{-1}$  and  $1080\text{ cm}^{-1}$  was around 2.46. The SERS spectra of the mixture of 4-MBA and 2-MPY are more complex than their respective SERS spectra. The spectra information from the cotton gauze-Ag SERS security label could be easily tuned by adjusting the ratio between 4-MBA and 2-MPY. The Raman spectra of mixture (2-MPY/4-MBA 10/1) was shown in Fig. 6(a), in which the Raman intensity ratio of the peaks at  $999\text{ cm}^{-1}$  and  $1080\text{ cm}^{-1}$  was around 2.36. After adjusting the component ratio to 1:5, the shape of the Raman spectra changed significantly, in which the characteristic vibrational peak at  $1072\text{ cm}^{-1}$  of 4-MBA was dominant in the spectra. Furthermore, the ratio of the peaks at  $999\text{ cm}^{-1}$  and  $1072\text{ cm}^{-1}$  was decreased to 0.30. Without the knowledge of molecular selection and their ratio, it would be extremely challenging for counterfeiters to analyze the SERS spectra and to fake the sample.

In order to further validate the versatile feasibility of the strategy proposed in this research, another typical Raman probe molecule PATP was employed to construct mixture with 2-MPY. The mixture of 2-MPY and PATP were self-assembled on the surface of the cotton gauze-Ag. The tunable encoding information was obtained by adjusting the ratio between 2-MPY and PATP as shown in Fig. 6 (b). The Raman intensity ratio of the peaks at  $999\text{ cm}^{-1}$  and  $1073\text{ cm}^{-1}$  decreased gradually as the ratio of 2-MPY/PATP decreases in mixture. The results indicated that the multi-molecule labeled plasmonic cotton gauze could provide high-level security information in anti-counterfeiting SERS security labels.

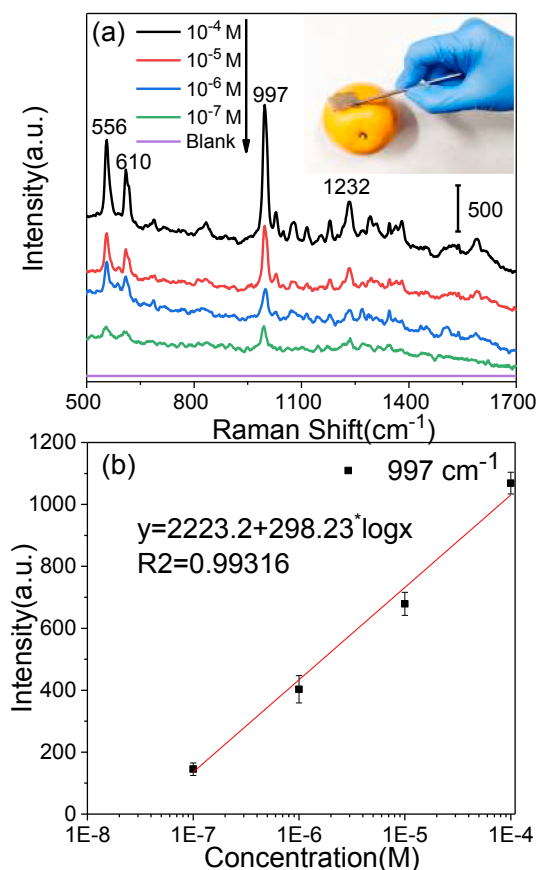


Fig. 5. Detection of the PMT from the surface of orange using cotton gauze-Ag as SERS substrate.

### 3.4. Practical anti-counterfeiting applications as wearable sensors

To demonstrate the feasibility of the plasmonic cotton gauze for practical anti-counterfeiting applications with tunable encoding information, the plasmonic cotton gauze labeled with multiple molecules was firstly sewed on a lab coat for on-site anti-counterfeiting investigations. The SERS spectra were collected on-site by a portable Raman spectrometer as shown in Fig. 7, in which the Raman intensity ratio of the peaks at  $999\text{ cm}^{-1}$  and  $1073\text{ cm}^{-1}$  was 1.5. The plasmonic cotton gauze was also glued on the surface of a package and used as anti-counterfeiting SERS security labels. After changing the proportion of 2-MPY/PATP in mixture the SERS spectra was changed significantly as presented in Fig. 7. The results indicated that the SERS security labels proposed at here can be widely adopted in many practical applications.

## 4. Conclusions

In summary, we have demonstrated a new type of anti-counterfeiting security labels based on plasmonic cotton gauze-Ag NPs composite, which was constructed by in-situ growth of high-density Ag NPs on the cotton gauze. The encoding SERS information of the security labels was complex and tunable, which was realized by adjusting the ratio between two Raman probe molecules modified on the plasmonic cotton gauze. Therefore, the feature information that was encrypted within the plasmonic SERS security labels cannot be cloned easily. As a proof-of-concept demonstration, the cotton gauze-Ag NPs were labeled with multiplex Raman reporters (2-MPY/PATP) and used as wearable anti-counterfeiting labels. After adjusting the coding information, the plasmonic cotton gauze was successfully glued onto the package and used as anti-counterfeiting labels. The fabricated plasmonic cotton gauze also shows excellent flexible features and SERS enhancement, which was

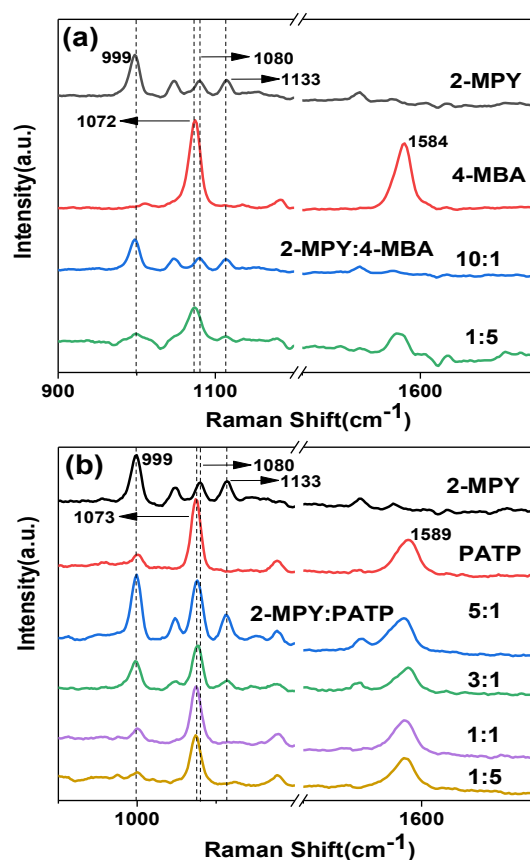


Fig. 6. Raman spectra of plasmonic cotton gauze labeled with 2-MPY/4-MBA (a) and 2-MPY/PATP(b) at different ratios.

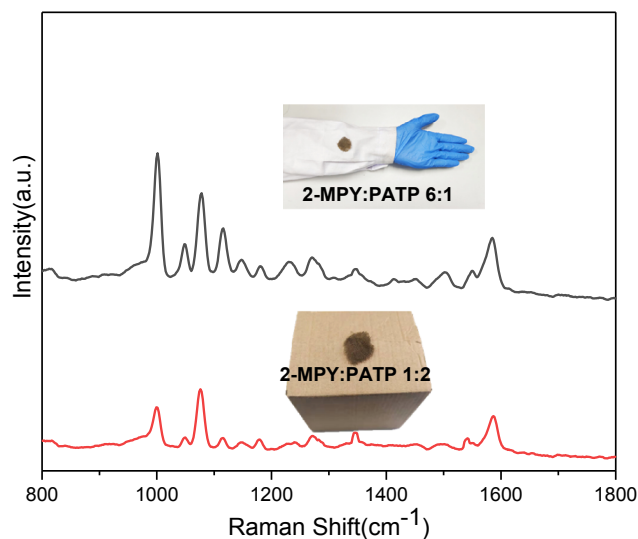


Fig. 7. Practical application of plasmonic cotton gauze as anti-counterfeiting SERS security labels.

used for SERS sensing of pesticide by simply swiping from the surface of oranges. The multi-functional plasmonic fabrics have a great potential for large-scale product labeling with effective anti-counterfeiting SERS security labels by unique tunable encoding information. In the meanwhile, the flexible SERS substrates can be applied to detecting pesticide residues by simply swiping from the surface of fruits.

## CRedit authorship contribution statement

**Sijia Liu:** Investigation, Writing – original draft. **Xiaoran Tian:** Investigation, Writing – original draft. **Jiaqi Guo:** Writing – review & editing. **Xianming Kong:** Conceptualization, Supervision. **Lingzi Xu:** Resources. **Qian Yu:** Conceptualization, Supervision. **Alan X. Wang:** Writing – review & editing.

## Declaration of Competing Interest

The authors declare that they have no known competing financial interests or personal relationships that could have appeared to influence the work reported in this paper.

## Acknowledgement

The authors would like to acknowledge the support from the Science Research Project of Education Department of Liaoning Province of China (No. L2019011), the United States National Institutes of Health (No. 1R21DA0437131) and the United States Department of Agriculture under (2017-67021-26606), and the talent scientific research fund of LSHU (No. 2017XJJ-037).

## Appendix A. Supplementary material

Supplementary data to this article can be found online at <https://doi.org/10.1016/j.apsusc.2021.150861>.

## References

- [1] R. Zhang, Y. Zhang, Z.C. Dong, S. Jiang, C. Zhang, L.G. Chen, L. Zhang, Y. Liao, J. Aizpurua, Y. Luo, J.L. Yang, J.G. Hou, Chemical mapping of a single molecule by plasmon-enhanced Raman scattering, *Nature* 498 (2013) 82–86.
- [2] Z. Gong, H. Du, F. Cheng, C. Wang, C. Wang, M. Fan, Fabrication of SERS swab for direct detection of trace explosives in fingerprints, *ACS Appl. Mater. Interfaces* 6 (2014) 21931–21937.
- [3] M. Fan, Z. Zhang, J. Hu, F. Cheng, C. Wang, C. Tang, J. Lin, A.G. Brolo, H. Zhan, Ag decorated sandpaper as flexible SERS substrate for direct swabbing sampling, *Mater. Lett.* 133 (2014) 57–59.
- [4] L.A. Lane, X. Qian, S. Nie, SERS Nanoparticles in Medicine: From Label-Free Detection to Spectroscopic Tagging, *Chem. Rev.* 115 (2015) 10489–10529.
- [5] H. Zhang, M. Liu, F. Zhou, D. Liu, G. Liu, G. Duan, W. Cai, Y. Li, Physical deposition improved SERS stability of morphology controlled periodic micro/nanostructured arrays based on colloidal templates, *Small* 11 (2015) 844–853.
- [6] K. Sivashanmugan, K. Squire, A. Tan, Y. Zhao, J.A. Kraai, G.L. Rorrer, A.X. Wang, Trace Detection of Tetrahydrocannabinol in Body Fluid via Surface-Enhanced Raman Scattering and Principal Component Analysis, *ACS Sensors* 4 (2019) 1109–1117.
- [7] K. Sivashanmugan, K. Squire, J.A. Kraai, A. Tan, Y. Zhao, G.L. Rorrer, A.X. Wang, Biological Photonic Crystal-Enhanced Plasmonic Mesocapsules: Approaching Single-Molecule Optofluidic-SERS Sensing, *Adv. Opt. Mater.* 7 (2019) 1900415.
- [8] S. Lin, X. Lin, Y. Shang, S. Han, W. Hasi, L. Wang, Self-Assembly of Faceted Gold Nanocrystals for Surface-Enhanced Raman Scattering Application, *The Journal of Physical Chemistry C* 123 (2019) 24714–24722.
- [9] W. Ji, L. Li, W. Song, X. Wang, B. Zhao, Y. Ozaki, Enhanced Raman scattering by ZnO superstructures: synergistic effect of charge transfer and Mie resonances, *Angew. Chem. Int. Ed.* 58 (2019) 14452–14456.
- [10] J. Chen, Y. Huang, P. Kannan, L. Zhang, Z. Lin, J. Zhang, T. Chen, L. Guo, Flexible and Adhesive Surface Enhance Raman Scattering Active Tape for Rapid Detection of Pesticide Residues in Fruits and Vegetables, *Anal. Chem.* 88 (2016) 2149–2155.
- [11] M. Park, C.S.H. Hwang, K.-H. Jeong, Nanoplasmonic Alloy of Au/Ag Nanocomposites on Paper Substrate for Biosensing Applications, *ACS Appl. Mater. Interfaces* 10 (2018) 290–295.
- [12] L.-L. Qu, Y.-Y. Geng, Z.-N. Bao, S. Riaz, H. Li, Silver nanoparticles on cotton swabs for improved surface-enhanced Raman scattering, and its application to the detection of carbaryl, *Microchim. Acta* 183 (2016) 1307–1313.
- [13] S.K. Bhunia, L. Zeiri, J. Manna, S. Nandi, R. Jelinek, Carbon-Dot/Silver-Nanoparticle Flexible SERS-Active Films, *ACS Appl. Mater. Interfaces* 8 (2016) 25637–25643.
- [14] S.A. Ogundare, W.E. van Zyl, A review of cellulose-based substrates for SERS: fundamentals, design principles, applications, *Cellulose* 26 (2019) 6489–6528.
- [15] Y. Chen, F. Ge, S. Guang, Z. Cai, Self-assembly of Ag nanoparticles on the woven cotton fabrics as mechanical flexible substrates for surface enhanced Raman scattering, *J. Alloy. Compd.* 726 (2017) 484–489.
- [16] S. Liu, R. Cui, Y. Ma, Q. Yu, A. Kannegulla, B. Wu, H. Fan, A.X. Wang, X. Kong, Plasmonic cellulose textile fiber from waste paper for BPA sensing by SERS, *Spectrochim. Acta Part A Mol. Biomol. Spectrosc.* 227 (2020) 117664.
- [17] B. Yoon, J. Lee, I.S. Park, S. Jeon, J. Lee, J.-M. Kim, Recent functional material based approaches to prevent and detect counterfeiting, *J. Mater. Chem. C* 1 (2013).
- [18] L. Lei, D. Chen, C. Li, F. Huang, J. Zhang, S. Xu, Inverse thermal quenching effect in lanthanide-doped upconversion nanocrystals for anti-counterfeiting, *J. Mater. Chem. C* 6 (2018) 5427–5433.
- [19] Y. Wang, L. Lei, R. Ye, G. Jia, Y. Hua, D. Deng, S. Xu, Integrating Positive and Negative Thermal Quenching Effect for Ultrasensitive Ratiometric Temperature Sensing and Anti-counterfeiting, *ACS Appl. Mater. Interfaces* (2021).
- [20] D. Peng, Q. Ju, X. Chen, R. Ma, B. Chen, G. Bai, J. Hao, X. Qiao, X. Fan, F. Wang, Lanthanide-doped energy cascade nanoparticles: full spectrum emission by single wavelength excitation, *Chem. Mater.* 27 (2015) 3115–3120.
- [21] X. Dai, K. Wang, L. Lei, S. Xu, Y. Cheng, Y. Wang, Pumping-controlled multicolor modulation of upconversion emission for dual-mode dynamic anti-counterfeiting, *Nanophotonics* 9 (2020) 1519–1528.
- [22] Y. Cui, R.S. Hegde, I.Y. Phang, H.K. Lee, X.Y. Ling, Encoding molecular information in plasmonic nanostructures for anti-counterfeiting applications, *Nanoscale* 6 (2014) 282–288.
- [23] Y. Liu, Y.H. Lee, Q. Zhang, Y. Cui, X.Y. Ling, Plasmonic nanopillar arrays encoded with multiplex molecular information for anti-counterfeiting applications, *J. Mater. Chem. C* 4 (2016) 4312–4319.
- [24] Y. Zheng, C. Jiang, S.H. Ng, Y. Lu, F. Han, U. Bach, J.J. Gooding, Unclonable Plasmonic Security Labels Achieved by Shadow-Mask-Lithography-Assisted Self-Assembly, *Adv. Mater.* 28 (2016) 2330–2336.
- [25] H. Cheng, Y. Lu, D. Zhu, L. Rosa, F. Han, M. Ma, W. Su, P.S. Francis, Y. Zheng, Plasmonic nanopapers: flexible, stable and sensitive multiplex PUF tags for unclonable anti-counterfeiting applications, *Nanoscale* 12 (2020) 9471–9480.
- [26] X. Kong, X. Chong, K. Squire, A.X. Wang, Microfluidic diatomite analytical devices for illicit drug sensing with ppb-level sensitivity, *Sens. Actuators, B* 259 (2018) 587–595.
- [27] X. Kong, Y. Xi, P. Le Duff, X. Chong, E. Li, F. Ren, G.L. Rorrer, A.X. Wang, Detecting explosive molecules from nanoliter solution: A new paradigm of SERS sensing on hydrophilic photonic crystal biosilica, *Biosens. Bioelectron.* 88 (2017) 63–70.
- [28] Y. Chen, F. Ge, S. Guang, Z. Cai, Low-cost and large-scale flexible SERS-cotton fabric as a wipe substrate for surface trace analysis, *Appl. Surf. Sci.* 436 (2018) 111–116.
- [29] L. Xia, M. Xu, G. Cheng, L. Yang, Y. Guo, D. Li, D. Fang, Q. Zhang, H. Liu, Facile construction of Ag nanoparticles encapsulated into carbon nanotubes with robust antibacterial activity, *Carbon* 130 (2018) 775–781.
- [30] D. Cheng, X. Bai, M. He, J. Wu, H. Yang, J. Ran, G. Cai, X. Wang, Polydopamine-assisted immobilization of Ag@AuNPs on cotton fabrics for sensitive and responsive SERS detection, *Cellulose* 26 (2019) 4191–4204.
- [31] Z. Liu, L. Cheng, L. Zhang, C. Jing, X. Shi, Z. Yang, Y. Long, J. Fang, Large-area fabrication of highly reproducible surface enhanced Raman substrate via a facile double sided tape-assisted transfer approach using hollow Au-Ag alloy nanourchins, *Nanoscale* 6 (2014) 2567–2572.
- [32] P. Lu, Y.-L. Hsieh, Preparation and properties of cellulose nanocrystals: Rods, spheres, and network, *Carbohydr. Polym.* 82 (2010) 329–336.
- [33] D. Cheng, M. He, J. Ran, G. Cai, J. Wu, X. Wang, Depositing a flexible substrate of triangular silver nanoplates onto cotton fabrics for sensitive SERS detection, *Sens. Actuators, B* 270 (2018) 508–517.
- [34] X. Kong, Q. Yu, X. Zhang, X. Du, H. Gong, H. Jiang, Synthesis and application of surface enhanced Raman scattering (SERS) tags of Ag@ SiO<sub>2</sub> core/shell nanoparticles in protein detection, *J. Mater. Chem.* 22 (2012) 7767–7774.
- [35] A. Cabrera Reina, S. Miralles-Cuevas, J.L. Casas López, J.A. Sánchez Pérez, Pyrimethanil degradation by photo-Fenton process: Influence of iron and irradiance level on treatment cost, *Sci. Total Environ.* 605–606 (2017) 230–237.
- [36] L. Mandrile, A. Giovannozzi, F. Durbiano, G. Martra, A. Rossi, Rapid and sensitive detection of pyrimethanil residues on pome fruits by Surface Enhanced Raman Scattering, *Food Chem.* 244 (2018) 16–24.